3 1176 00073 4666

UNCLASSIFIED Reference #43

~~CONFIDENTIAL~~

NASA TECHNICAL MEMORANDUM

NASA TM X-1049

C5

NASA TM X-1049

CLASSIFICATION CHANGE
TO UNCLASSIFIED
By Authority of NASA ltr dtd Oct. 21, 1969 / s/ Jacob E. Smart
Initial/Date AVS 9/20/2004

EFFECTS OF EXTERNAL MATERIAL INJECTION ON RADIO-SIGNAL TRANSMISSION THROUGH A ROCKET EXHAUST

by Duncan E. McIver, Jr., W. Linwood Jones, and William F. Cuddihy

Langley Research Center
Langley Station, Hampton, Va.

NATIONAL AERONAUTICS AND SPACE ADMINISTRATION • WASHINGTON, D. C. • JANUARY 1965

~~CONFIDENTIAL~~

UNCLASSIFIED

EFFECTS OF EXTERNAL MATERIAL INJECTION ON RADIO-SIGNAL TRANSMISSION THROUGH A ROCKET EXHAUST

By Duncan E. McIver, Jr., W. Linwood Jones, and William F. Cuddihy

Langley Research Center
Langley Station, Hampton, Va.

NATIONAL AERONAUTICS AND SPACE ADMINISTRATION

EFFECTS OF EXTERNAL MATERIAL INJECTION ON RADIO-SIGNAL TRANSMISSION THROUGH A ROCKET EXHAUST*

By Duncan E. McIver, Jr., W. Linwood Jones,
and William F. Cuddihy
Langley Research Center

SUMMARY

Ground experiments were conducted at the Langley Research Center to determine the effectiveness of water and freon injection into the exhaust of a static fired full-scale solid-propellant rocket motor for the purpose of eliminating radio-frequency (RF) signal interference. These materials were injected at varying flow rates into the exhaust of an Altair-IIB1 rocket motor. During these tests, X-band microwave transmission, C-band plasma noise, and relative luminosity (in the 0.65- to 1.00-micron region) were recorded. The motor uses a double base highly aluminized solid propellant with a mass flow of about 22 pounds per second. Preliminary analysis of the results indicates that at a position of 101 inches downstream of the nozzle, prior to material injection, the X-band signal experienced attenuation in excess of 53 decibels, C-band radiation from the exhaust indicated about a 2000° K effective antenna noise (ambient level about 290° K) which represents an 8-decibel degradation in receiver sensitivity, and the radiant intensity showed a marked increase over the ambient level. When water was injected into the exhaust 3 inches downstream from the nozzle, these effects were reduced or completely eliminated, depending upon the mass flow of the injectant.

INTRODUCTION

The free exhaust jets of solid-propellant rocket motors can cause several undesirable effects; two are: the attenuation of radar and telemetry signals and the radiation of electromagnetic signals over a broad frequency range. These phenomena are caused by various chemical and fluid dynamic processes in the exhaust.

The problem that has received the most attention is the interference of electromagnetic signals (refs. 1, 2, and 3) and was the theme of the American Rocket Society "Conference on Ions in Flames and Rocket Exhausts," held in Palm Springs, California in October 1962. This interference, which includes

---

*Title, Unclassified.

both attenuation of transmitted signals and increased "effective" antenna noise temperature of onboard receiving systems (such as radar transponders), is attributed to free electrons, which have been created by ionization processes in the combustion chamber and the exhaust. In some cases the interference is severe enough to completely disrupt vital communication links.

The optical radiation emitted from the exhaust creates several problems for the ballistic missile system. Using radiation detection schemes in satellites, the enemy can detect a missile during the launch phase; thus, the surprise element is eliminated. The radiation may also interfere with vehicle-borne optical guidance equipment.

The Langley Research Center is currently investigating the effects of rocket exhausts on radio-frequency (RF) signal systems (refs. 2, 3, and 4). As part of the program, tests were conducted during the static firing of a new Scout fourth-stage rocket motor to determine the effectiveness of injecting water and freon into the exhaust to reduce the unwanted electromagnetic signal attenuation and radiation effects. This report presents a brief discussion of theoretical considerations, experimental apparatus, and test results.

THEORETICAL CONSIDERATIONS

Free Electron Generation and Distribution

Some of the sources of electrons are, according to reference 5, ionization processes in the combustion chamber, afterburning on the exhaust surface, ablation and subsequent ionization of nozzle material, and shock ionization in the exhaust. Thermal ionization of alkali metal impurities is generally attributed to be the prime source of electrons in the exhausts of solid-propellant rocket motors. The distribution of electrons in the exhaust will depend on which of the ionization processes is predominant, the various rate constants of ionization and de-ionization, and the fluid dynamics of the exhaust gases.

Electromagnetic Energy Interaction With a Plasma

The rocket exhaust is an inhomogeneous plasma which can absorb, reflect, and shift the phase of electromagnetic signals which are transmitted through it. The degree of interaction depends on the signal frequency and the electron density and collision frequency along the signal path. Several detailed discussions of this interaction are available in references 5 to 8 and some of the basic elements are presented in the appendix.

Optical and Radio-Frequency Radiation From the Exhaust Plasma

The high temperature gases and particles in the exhaust will generate electromagnetic radiation over a wide frequency range (refs. 9 and 10). The processes of radiation are probably Bremsstrahlung (braking of electrons in the coulomb field of atoms), electronic excitation of atoms and molecules, and black body from the incandescent solid particles. The intensity of the radiation is a function of the temperature of the exhaust constituents.

De-ionization and De-excitation by External Injection

Two processes which reduce the electron level in a plasma are recombination and attachment (ref. 5). Injecting liquids with large heat capacities or attachment coefficients into an exhaust will enhance these processes by cooling and electrophilic action. If sufficient quantity of injectant is employed, undesirable radio-frequency (RF) signal interference and radiation can be eliminated. In cases where afterburning is the prime source of attenuation and radiation, the injectant can be used for quenching (refs. 2, 3, and 11).

Water and freon $\left(CCl_2F_2\right)$ are attractive materials since they can be injected in liquid form, thus increasing the probability of penetration into the exhaust (ref. 4). Since water has a large heat capacity and latent heat (1000 Btu/lb), it is an efficient coolant. Freon has two constituents: chlorine and fluorine, in the halogen family, which are electrophilic. The halogens have often been suggested as additives for reducing electron concentrations (ref. 5). Some doubts have been raised, however, concerning the effectiveness of halogens for this purpose (ref. 12).

EXPERIMENTAL APPARATUS

The overall experimental setup for the material-injection tests is shown in figure 1. The material-injection point was 3 inches downstream of the nozzle with electromagnetic sensing devices located about 101 inches or about 16 nozzle diameters further downstream. These positions were arbitrarily chosen to be compatible with the motor test setup.

Rocket Motor and Setup

The Altair rocket motor, which uses a highly aluminized solid propellant, is an alternate fourth-stage motor for the Scout vehicle. For these tests, the motor was fired in a spinning rig (200 rpm) to simulate Scout flight conditions. Details of the propellant and motor operation are given in table I.

Material-Injection Systems

The plumbing arrangement for the water and the CCl_2F_2 (freon) systems is shown in figure 2. Each system was pressurized to 1000 psig at the beginning of the experiment. A regulator was employed to maintain constant pressure in the water system.

Six different size orifices, three sizes in each test, were used in the water system to achieve variable flow rates at constant pressure. The orifice arrangement, size, injection direction, and flow rates are shown in figure 3. Two directly opposed orifices of the same size were used for each flow rate. A typical nozzle installation is shown in figure 4.

In addition to the six fixed flow levels, variable flow rates were obtained for the larger orifices by the use of a hydraulically operated ball valve in the main feed line. For the smaller orifices (2 pounds per second or less in mass flow), this valve had little effect.

Only one set of orifices was used for the freon system and the orifice size and injection direction are shown in figure 3. The freon mass-flow rate of about 1.9 pounds per second was held relatively constant during the test by making the ratio of air to freon in the accumulator large (fig. 2). The flow rate was calibrated by measuring the weight loss for a given injection time.

The injection systems were operated by a programer which coordinated ball valve operation and solenoid operation. Periods of no-flow were provided for calibration purposes.

Microwave Transmission Instrumentation

The microwave attenuation and phase measuring system is shown schematically in figure 5 and the antenna installation is shown in figure 6. This system is a modified microwave bridge operating at X-band (9.23 Gc). The rocket exhaust (plasma) is introduced into the work path between the two focusing antennas and the change in received power is recorded. The antennas are conical horns with 12-inch-diameter polystyrene hyperbolic lenses. The energy is focused to approximately a 4-inch half-power spot diameter at a distance of 32.5 inches from the lens surface. Teflon slabs, 1/2 wavelength thick, to minimize reflections were used to protect the antenna lenses from heat generated by the exhaust The transmitted power and received power were monitored by crystal diode detectors calibrated with a precision attenuator.

The plasma insertion phase shift is measured by comparing the phase of the microwave signal in the work path with that of the signal in the reference path before and after plasma insertion. To accurately measure this phase shift, the RF signals of the two klystrons are frequency locked by use of synchronizers and then heterodyned in waveguide mixers to produce two 27-kc signals. These video signals are then fed to the precision phase meter and the magnetic tape recorder. The analog output of the phase meter is a d-c voltage proportional to the microwave phase. The amplitude of the 27-kc work-path signal is also employed to determine signal attenuation due to the plasma.

Microwave Radiation Instrumentation

The microwave radiation system consists of a C-band radiometer and a pyramidal horn antenna. The radiometer, essentially a microwave receiver with a switched RF input, operates at a fixed frequency of 5 Gc. The input is switched at 10 cycles per second between the antenna terminals and a matched load at ambient temperature (about 290° K). The output of the radiometer appears as a square wave whose amplitude represents the difference between the effective antenna noise temperature T_A and the reference temperature T_R. A block diagram of the system is shown in figure 7. The radiometer was calibrated with a standard noise source.

Optical Instrumentation

An unfiltered photomultiplier with a 3-inch objective lens was employed to sense the radiant intensity of the exhaust. The sensor recorded the relative intensity in the wavelength region from 0.65 to 1 micron. The sensor was located about 30 feet from the exhaust axis (fig. 1) and viewed the region just downstream of the microwave instrumentation. Its field of view, 2°, represents an area of about 1 square foot, which was smaller than the visible exhaust.

RESULTS

Motor Operation and Material-Injection System

For the two tests, operation of the rocket motor was considered normal and burning times and chamber conditions followed closely the values given in table I.

The water and freon flow rates for the two tests are presented in figure 8.

Electromagnetic Measurements

The three electromagnetic measurements, transmission of microwave signals at X-band, detection of radiation at C-band, and detection of radiation in the 0.65- to 1-micron region were obtained during both motor firings. Samples of the data from these measurements are shown in figure 9 correlated with water flow data.

<u>Microwave transmission data</u>.- At motor ignition, the attenuation of 9.23 Gc signals was in excess of 53 decibels. Some signal recovery (10 decibels) was noticed when the mass flow of the water exceeded 1 pound per second, and full recovery was achieved when the water flow was about 11 pounds per second. The direction of injection appeared to have little effect on the amount of signal recovery.

Phase measurements correlated with the attenuation data in terms of recovery; however, accurate phase measurements were only possible when the signal attenuation was less than 50 decibels. The measured phase shift when the signal was attenuated 43 decibels was 91°.

Due to a valve malfunction, the freon was injected with a continuous flow of about 2 pounds per second of water. The combined total of water and freon mass flow appeared to cause about the same degree of recovery for an equivalent amount of water alone.

Attenuation data from both tests have been plotted in figure 10 to show the the reduction in attenuation as a function of injectant mass-flow rate w_I expressed as a percentage of rocket exhaust mass-flow rate w_R. Significant reduction (about 25 decibels) is evident for values as low as 10 percent and complete reduction occurred when value was about 50 percent. The accuracy of the attenuation data is considered to be ±2 percent of the measured value.

The values plotted are given in table II and show the relationship between injectant angle θ and amounts of water and freon. As seen in figure 10, a smooth curve can be fitted to data from both injection angles for water and for the case of freon plus water.

The same values are plotted on semilogarithmic paper in figure 11 and show almost a straight line relationship between the logarithm of attenuation and injectant flow. This relationship indicates an exponential dependence of attenuation on material injectant.

Values of the average electron density and collision frequency, for a typical flow interval, were calculated by the technique described in the appendix and are shown in figure 12.

Microwave radiation data.- For test 1, the radiometer indicated an increase in effective antenna noise temperature to 2000° K (ambient level about 290° K) which represents an 8-decibel loss in receiver sensitivity at C-band. At maximum water flow (injectant flow rate of about 41 percent of exhaust flow rate), the noise temperature returned to the ambient level. Equipment malfunction during test 2 prevented a quantitative analysis of the noise data as a function of flow.

Optical data.- A marked increase in optical radiation above the ambient level occurred during motor operation. Water injection, at the maximum flow rate, caused almost full reduction (90 to 95 percent) of the radiation measured at the 101-inch position. Since calibration of the absolute radiation level was not available, only relative intensity plotted against percent of injectant to propellant mass flow is presented. (See fig. 13.) These limited data indicate that more efficient recovery occurs when water is injected at 90°. The freon had no detectable effect on the radiation.

Motion pictures obtained of the exhaust during the tests clearly show the change in radiant intensity during water injection. (See fig. 14.)

DISCUSSION

The results of these tests show that the addition of material may hold some promise as a possible technique to overcome the undesirable electromagnetic interference due to a solid-propellant rocket exhaust. Since this report is primarily a description of test results, no detailed analysis of the processes involved will be attempted; however, the mechanisms of de-ionization and de-excitation are probably recombination and attachment as a result of cooling and electrophilic action as previously mentioned. Afterburning of the exhaust products with entrained air is one source of ionization and radiation and the injected material, especially water, will quench this secondary combustion.

The concept of material addition to eliminate VHF signal attenuation was suggested early by the flight results of the Scout vehicle (refs. 2 and 3). During the operation of the second-stage motor, a small amount of decomposed hydrogen peroxide from attitude control jets which was injected into the second-stage motor exhaust eliminated VHF signal attenuation. The ratio of injectant to propellant mass flow was about 0.014. The attenuation was attributed to afterburning and the signal recovery to quenching by water vapor (a constituent of decomposed hydrogen peroxide).

In ground tests at the Langley Research Center, water ejected from a nose cone immersed in the exhaust of a solid-propellant rocket motor was effective in reducing RF signal attenuation (ref. 4). Other ground tests at the Lewis Research Center (ref. 13) and at the U.S. Naval Research Laboratory (ref. 14) have demonstrated the feasibility of material addition for reducing the electron concentration.

A recent flight test (ref. 15) based on the preceding ground tests has demonstrated that material addition is a practical solution to the radio attenuation problem incurred during hypersonic flight. Water was injected into the flow field at the stagnation point and near the antenna locations and was effective in reducing attenuation.

The application of this technique for the reduction of exhaust-induced attenuation is particularly suitable when changes in propellant composition, radio signal frequency, or ground station location are not possible (ref. 3). For minimizing exhaust radiation, material additions would be helpful when propellant composition cannot be changed. Although the data presented herein indicate the feasibility of the material-addition concept, they are not complete enough for application to specific flight missions. Additional tests are needed to determine the optimum material and injection technique. The effect of altitude should also be determined; for example, only a small amount of material (1.4 percent) was needed to eliminate exhaust attenuation of the Scout second-stage motor in flight (ref. 2).

CONCLUDING REMARKS

Preliminary results from experiments conducted at the Langley Research Center in which water and freon were injected into the exhaust of a solid-propellant rocket motor to reduce electromagnetic interference effects indicate that a marked reduction of the X-band attenuation and C-band radiation can be achieved. Significant signal recovery was observed when the injectant mass-flow rate was 10 percent of the rocket exhaust mass-flow rate; almost complete signal recovery was observed when the value was about 50 percent. Optical radiation was reduced 80 to 90 percent when water was injected at 50 percent exhaust mass-flow rate. No detailed analysis of the processes involved and no extrapolation of the data to flight missions are presented. Additional studies are recommended.

Langley Research Center,
National Aeronautics and Space Administration,
Langley Station, Hampton, Va., May 28, 1964.

APPENDIX

DETERMINATION OF ELECTRON DENSITY AND COLLISION FREQUENCY IN A PLASMA BY MICROWAVE TRANSMISSION

The following symbols are used in this appendix:

A	total or measured attenuation, αd, dB
c	velocity of light, 3×10^8 m/sec
d	plasma thickness, cm
N_e	electron density, electrons/cm^3
α	attenuation coefficient, dB/cm
β	phase-shift coefficient, rad/cm
$\Delta\beta$	relative phase shift, rad/cm
β_0	free-space phase-shift coefficient, rad/cm (for 9.23 Gc, $\beta_0 = 1.932$)
γ	plasma propagation constant, cm^{-1}
λ	free-space wavelength, cm
ν	collision frequency, collisions/sec
ρ	power reflection coefficient
ϕ	total or measured phase shift, rad
ω	signal frequency, rad/sec (for 9.23 Gc, $\omega = 5.796 \times 10^{10}$)
ω_p	plasma resonant frequency, rad/sec

The following treatment is a simplified theoretical description of the interaction of electromagnetic waves with a plasma to show how the attenuation and phase shift data can be related to the intrinsic properties of the plasma, the electron density, and collision frequency.

For a given electron density there is an associated critical radio frequency called the plasma frequency as shown by the following expression:

$$\omega_p = 5.64 \times 10^4 \sqrt{N_e} \tag{1}$$

If normal-incidence plane-wave interaction with a homogeneous, semi-infinite plasma slab is assumed and the inequality

$$\left(\frac{\omega_p}{\omega}\right)^4 \ll 1 \tag{2}$$

is true, from reference 5 the complex propagation constant may be expressed in terms of the plasma properties in the following simplified form:

$$\gamma = \alpha + j\beta \tag{3}$$

where attenuation coefficient is

$$\alpha = \frac{8.686\nu\omega_p{}^2}{2C(\omega^2 + \nu^2)} \tag{4}$$

and the phase-shift coefficient is

$$\beta = \frac{2\pi}{\lambda}\left[1 - \frac{\omega_p{}^2}{2(\omega^2 + \nu^2)}\right] \tag{5}$$

the reflection coefficient (power) is

$$\rho = \frac{(\beta_0 - \beta)^2 + \alpha^2}{(\beta_0 + \beta)^2 + \alpha^2} \tag{6}$$

For diagnostic purposes, to determine both the electron density and the collision frequency, two measurements are necessary. The general procedure is to make attenuation measurements at two frequencies and solve for the two properties. An alternate approach is to measure both the attenuation and phase-shift coefficient at one frequency, which will yield the same results. When both α and β are measured, the following expression for collision frequency is obtained:

$$\nu = \frac{\beta_0 c\alpha}{8.686(\beta_0 - \beta)} \tag{7}$$

To obtain the average value of the electron density, the value of ν can then be substituted in the following expression:

$$N_e = \frac{1}{d(8.686)(3.178 \times 10^9)}\left[\frac{2c\alpha(\omega^2 + \nu^2)}{\nu}\right] \tag{8}$$

It can be seen from equation (7) that the collision frequency can be determined when the plasma propagation constant $\gamma = \alpha + j^{\beta}$ is known. If in equation (7) α were replaced by the total attenuation A (αd) and $(\beta_0 - \beta)$ were replaced by the total phase shift ϕ $\left((\beta_0 - \beta)d\right)$, then ν could be determined without knowing the plasma thickness, as shown in the following expression for an operating frequency of 9.23 Gc:

$$\nu = 6.67 \times 10^9 \frac{A}{\phi} \tag{9}$$

The electron density from equation (8) is, however, inversely proportional to the thickness; therefore, d must be determined. To calculate this parameter use is made of figures 15 and 16. Figure 15 was constructed by taking arbitrary values of N_e and ν and solving equations (7) and (8) for α and $\Delta\beta$ $\left(\text{where } \Delta\beta = \beta_0 - \beta\right)$. If the ratio $\alpha/\Delta\beta$ or A/ϕ is plotted as the ordinate and ν as the abscissa, a family of curves for constant N_e is generated. Figure 16 was constructed by calculating α or A/d for various values of N_e and ν.

To calculate the thickness, equation (7) was solved for ν and a vertical line was drawn on figures 15 and 16 for this value. The ratio A/ϕ was then determined and a horizontal line was drawn on figure 15. The intersection of these two lines determines the average electron density. The intersection of similar lines of ν and N_e on figure 16 yields a value of A/d which can be solved for the thickness d.

The following is a sample calculation:

(1) Measured attenuation A is 46 dB

(2) Measured phase shift ϕ is 1.48 rad

(3) $\frac{A}{\phi} = 31.1$

(4) From equation (9), $\nu = 6.67 \times 10^9(31.1) = 2.1 \times 10^{11}$

(5) From figure 15, $N_e \approx 2.5 \times 10^{11}$

(6) From figure 16, $\frac{A}{d} \approx 0.56$

(7) $d = \dfrac{(46)}{(0.56)2.54} \approx 32$ in.

REFERENCES

1. Anon.: Radar Attenuation Symposium. CPIA Pub. No. 6 (Contract NOw 62-0604-c), Appl. Phys. Lab., The Johns Hopkins Univ., Jan. 1963.

2. Sims, Theo E., and Jones, Robert F.: Rocket Exhaust Effects on Radio Frequency Propagation From a Scout Vehicle and Signal Recovery During the Injection of Decomposed Hydrogen Peroxide. NASA TM X-529, 1961.

3. McIver, Duncan E., Jr.: Study of the Effects of a Rocket Exhaust on Radio Frequency Signal Attenuation by the Use of a Recoverable Camera on the NASA Scout Vehicle. NASA TM X-888, 1963.

4. Cuddihy, W. F., and Hughes, J. Kenrick: Simulated Reentry Tests of a Method for Reducing Radio Blackout by Material Addition to Ionized Flow Field. NASA TM X-988, 1964.

5. Calcote, H. F., and Silla, H.: Radar Attenuation in Solid Propellant Rocket Exhausts. Bull. 18th Meeting JANAF-ARPA-NASA Solid Propellant Group, Vol. III, June 1962, pp. 3-50.

6. Huber, Paul W., and Nelson, Clifford H.: Plasma Frequency and Radio Attenuation. Proceedings of the NASA-University Conference on the Science and Technology of Space Exploration, Vol. 2, NASA SP-11, 1962, pp. 347-360. (Also available as NASA SP-25.)

7. Altshuler, S., Moe, M. M., and Molmud, P.: The Electromagnetics of the Rocket Exhaust. GM-TR-0165-00397, Space Technology Labs., Inc., June 15, 1958.

8. Swift, Calvin T., and Evans, John S.: Generalized Treatment of Plane Electromagnetic Waves Passing Through an Isotropic Inhomogeneous Plasma Slab at Arbitrary Angles of Incidence. NASA TR R-172, 1963.

9. Ritland, H. N., Capiaux, R., and Meyerott, R. E.: Radiation Emission Processes in Rocket Plumes. LMSC-B007317 (Contract No. Nonr-3559(00)), Lockheed Missiles & Space Co., Dec. 1962. (Available from ASTIA as 333600.)

10. Anon.: R-F Radiation From Rocket Flames. SEP Doc No. 126-11-30A (AFCRL-TR-60-166), Appl. Res. Lab., Sylvania Electronic Systems, June 24, 1960. (Available from ASTIA as AD 318842.)

11. Anon.: Infrared Countermeasures Research. Volume I - Introduction of Additives Into the Mixing Region To Suppress Afterburning. Rep. No. ZR-AP-061-25 (SSD-TR-61-19(I)), Gen. Dynamics/Astronautics, Feb. 1962. (Available from ASTIA as AD-328903.)

12. Padley, P. J., Page, F. M., and Sugden, T. M.: Effect of Halogens on the Ionization in Alkali-Laden Hydrogen and Acetylene Flames. Part I.- The Theory of Steady State Ionization in Flames. Trans. Faraday Soc., vol. 57, pt. 9, no. 465, Sept. 1961, pp. 1552-1562.

13. Kuhns, Perry W., and Cooper, Dale W.: Effect of Water Addition on Microwave Transmission Through a Cold Plasma Layer. NASA TM X-874, 1963.

14. Balwanz, W. W., and Stine, P. T.: The Plasmas of Missile Flight - Analysis of Polaris A2X Signal Absorption. NRL Rep. No. 5636, U.S. Naval Res. Lab., July 24, 1961.

15. Cuddihy, William F., Beckwith, Ivan E., and Schroeder, Lyle C.: RAM B2 Flight Test of a Method for Reducing Radio Attenuation During Hypersonic Reentry. NASA TM X-902, 1963.

UNCLASSIFIED

[redacted]

TABLE I.- ALTAIR-IIB1 MOTOR DATA

Propellant weight, lb	504.4
Thrust, lb:	
Average	4840
Maximum	5425
Specific impulse, sec:	
At sea level	220
In vacuum	278.5
Throat area, sq in.	8.08
Exit area, sq in.	31.55
Exit diameter, in.	6.35
Operation time, sec	22.7
Mass flow, lb/sec	22.1
Chamber pressure, psig:	
Maximum	455
Average	426
Chamber temperature, °F	6100
Nozzle half angle, deg	18

Propellant formulation:	Percent by weight
Nitrocellulose	22.3
Nitroglycerine	26.7
Aluminum	20.5
HMX	14.9
Ammonium perchlorate	7.4
TA	6.1
Resorcinol	1.1
NDPA	1.0

Exhaust gas composition (calculated):	Percent by volume
Al_2O_3	10.34
CO	39.20
CO_2	1.22
H_2	27.75
H_2O	4.80
N_2	14.45
HCl	1.70
H, Cl, OH, AlCl	0.54

[redacted] UNCLASSIFIED

TABLE II.- VALUES OF X-BAND ATTENUATION AND OF w_I/w_R

[Plotted in fig. 10]

w_I/w_R, percent, for -			Total w_I/w_R, percent	Total observed attenuation, dB ± 2%
Water at $\theta = 45^\circ$	Water at $\theta = 90^\circ$	Freon at $\theta = 90^\circ$		
0	0	0	0	53
2.2	0	0	2.2	53
2.5	0	0	2.5	53
4.0	0	0	4.0	46
5.4	0	0	5.4	41
5.6	0	0	5.6	43
11.3	0	0	11.3	29
11.4	0	0	11.4	27
11.4	0	0	11.4	25
7.1	4.1	0	11.2	24
6.8	7.2	0	14.0	18.5
8.6	9.5	0	18.1	12.5
11.0	0	8.6	19.6	12.0
18.5	4.1	8.6	31.2	5.5
34.0	0	0	34.0	5.0
35.6	0	0	35.6	5.5
0	39.3	0	39.3	2.5
25.5	5.4	8.6	39.5	3.2
0	41.1	0	41.1	2.5
0	43.0	0	43.0	1.6
11.3	36.2	0	47.5	8
10.5	37.6	0	48.1	1.2
24.6	16.3	8.6	49.5	1.0
26.8	18.1	8.6	53.5	.5
28.5	19.9	8.6	58.0	0
35.0	25.0	0	60.0	0
34.5	30.0	0	64.5	0

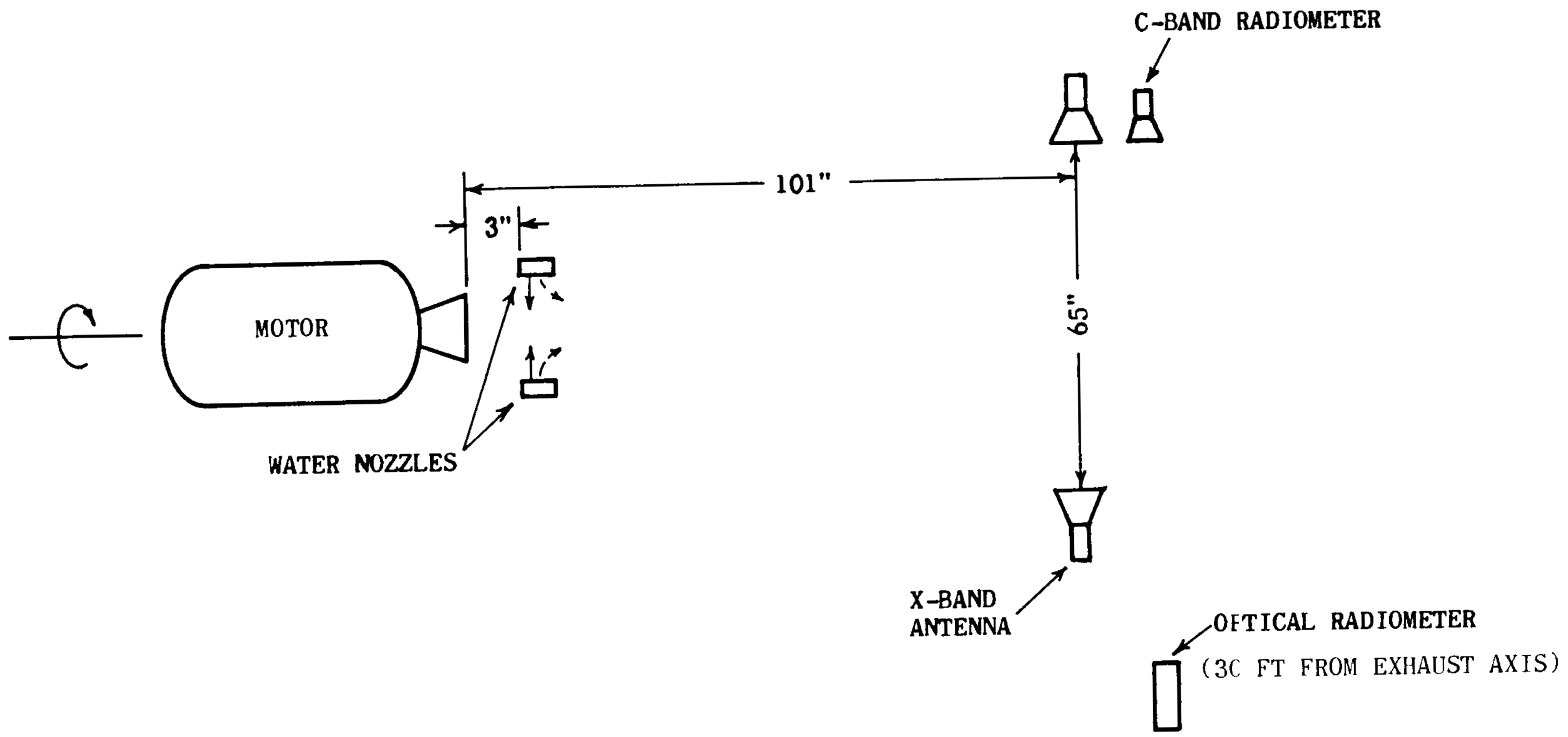

Figure 1.- Experimental setup for material-injection tests.

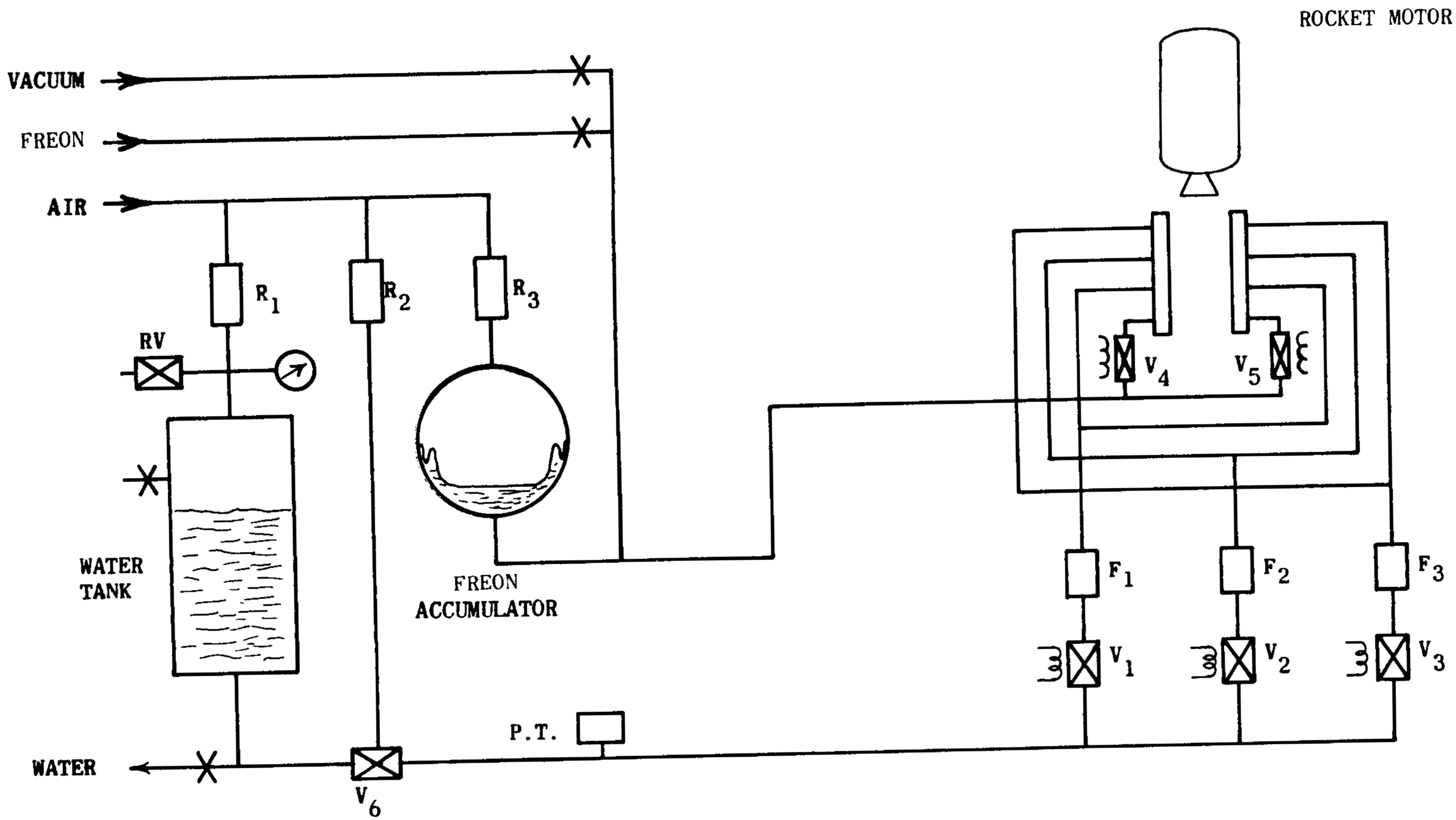

R1,R2,R3	**REGULATORS**
RV	**RELIEF VALVE**
PT	**PRESSURE TRANSDUCER**
V1,V2,V3	**SOLENOID VALVES, WATER SYSTEM**
V4,V5	**SOLENOID VALVES, FREON SYSTEM**
V6	**PNEUMATIC BALL VALVE**
F1,F2,F3	**FLOW METERS**

Figure 2.- Plumbing arrangement for water and CCl_2F_2 (freon) injection systems.

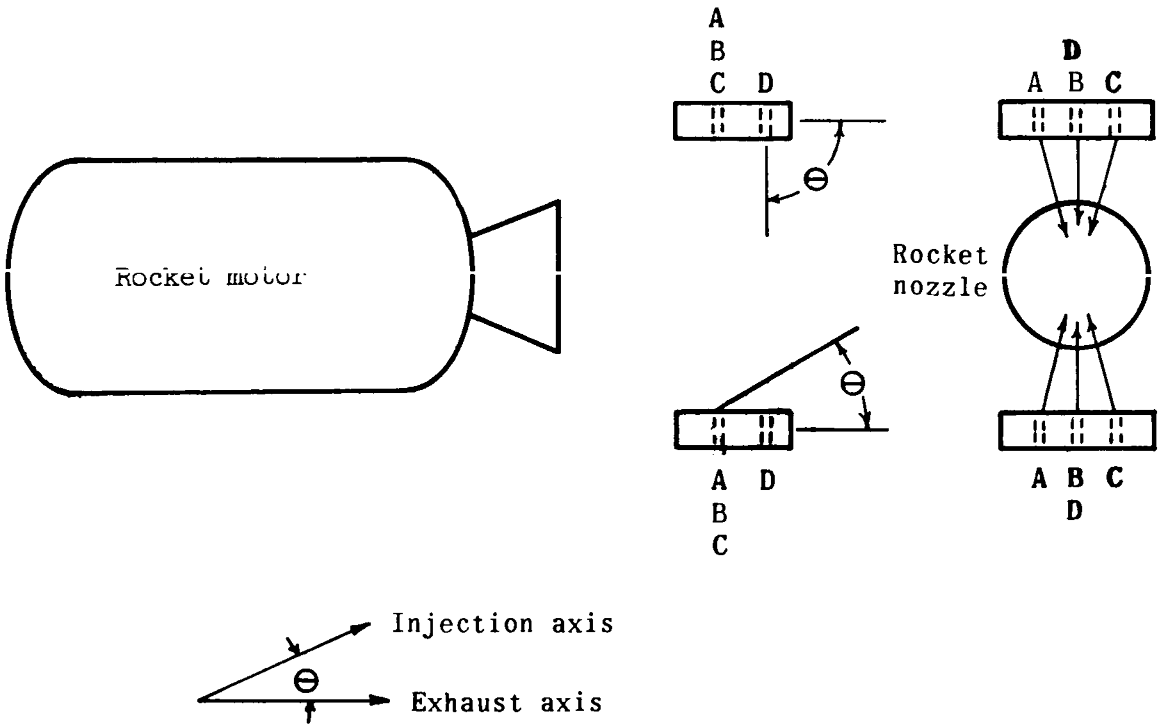

	Test 1			Test 2		
	Diameter, in.	w, lb/sec	θ, deg	Diameter, in.	w, lb/sec	θ, deg
A	0.0796	1	90	0.113	2	45
B	0.252	10	90	0.226	8	90
C	0.0252	0.1	90	0.178	5	45
Freon D	-----	---	---	0.138	2	90

Figure 3.- Orifice arrangement, size, injection directions, and flow rates for material-injection tests.

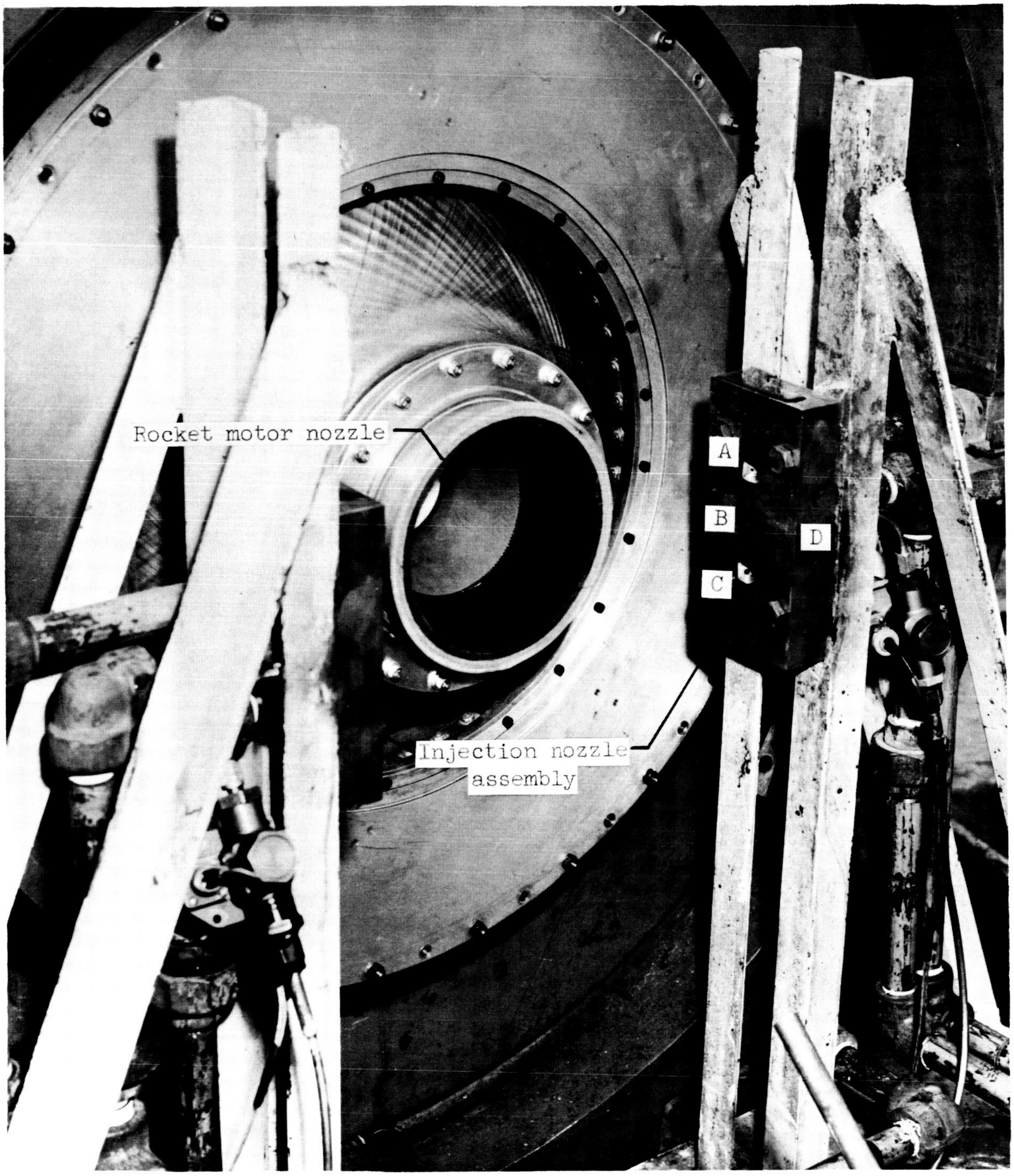

Figure 4.- A typical injection nozzle installation. L-63-5034.1

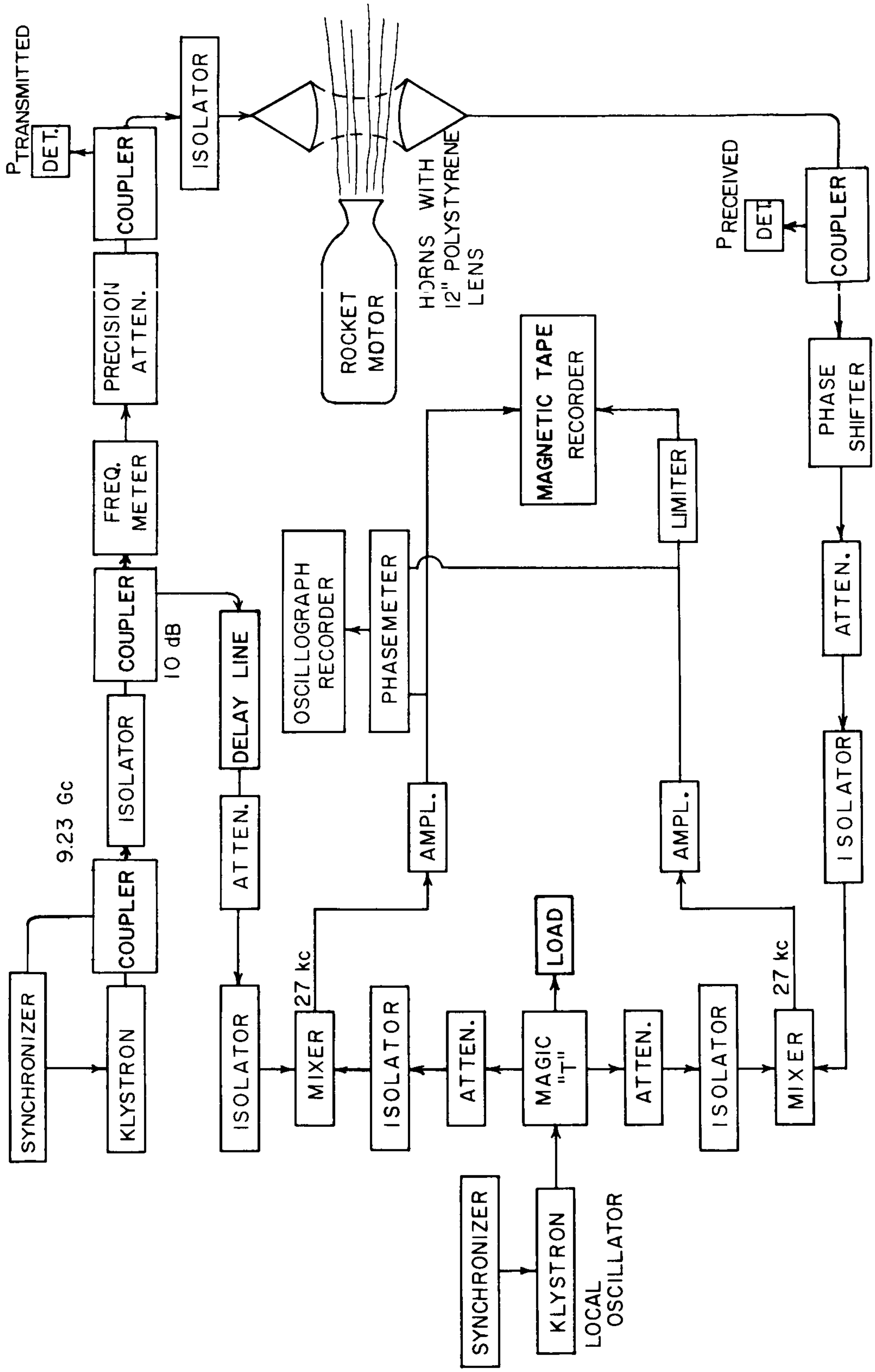

Figure 5.- Microwave attenuation and phase measuring system.

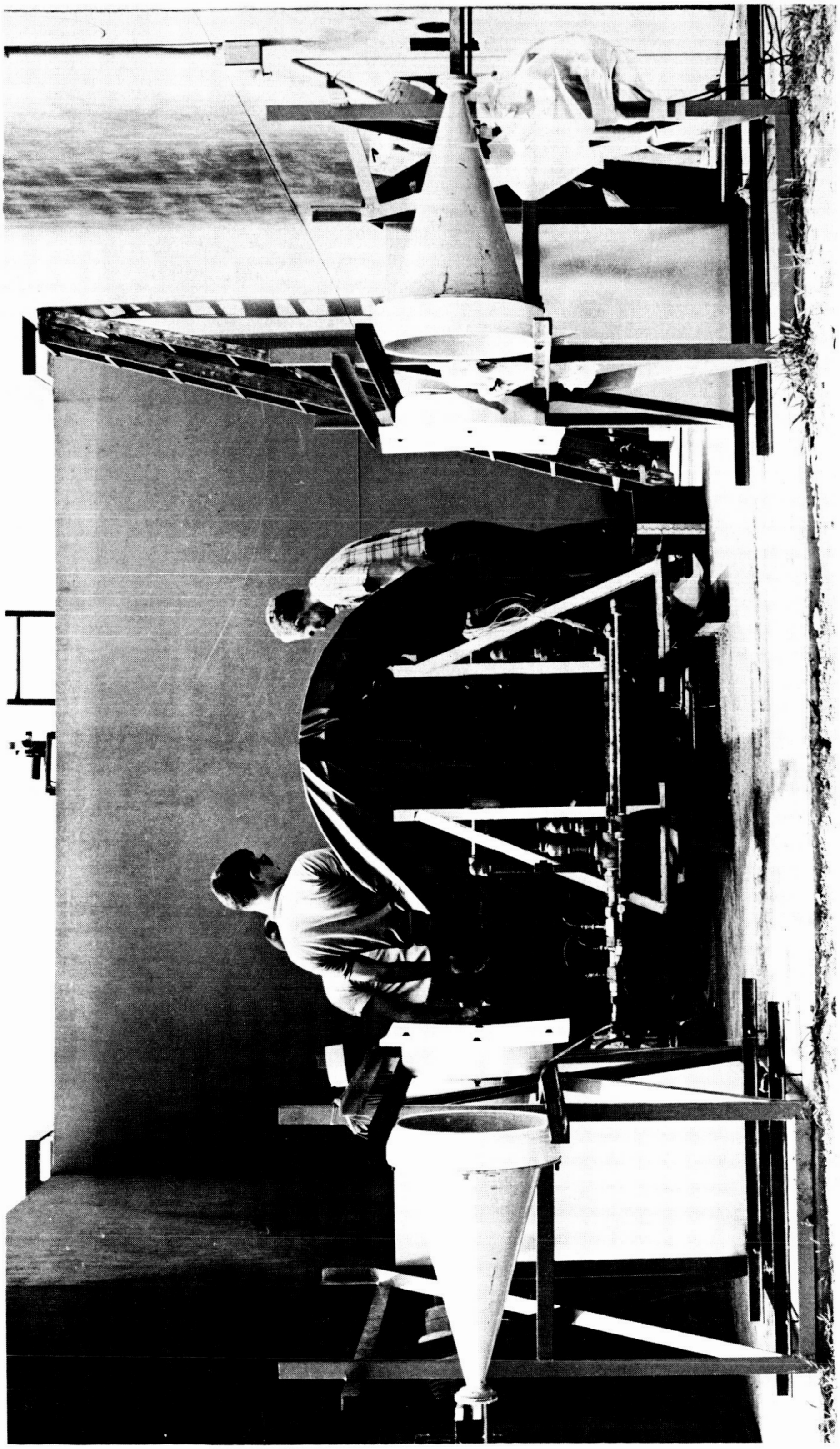

L-63-4569

Figure 6.- Typical microwave antenna installation.

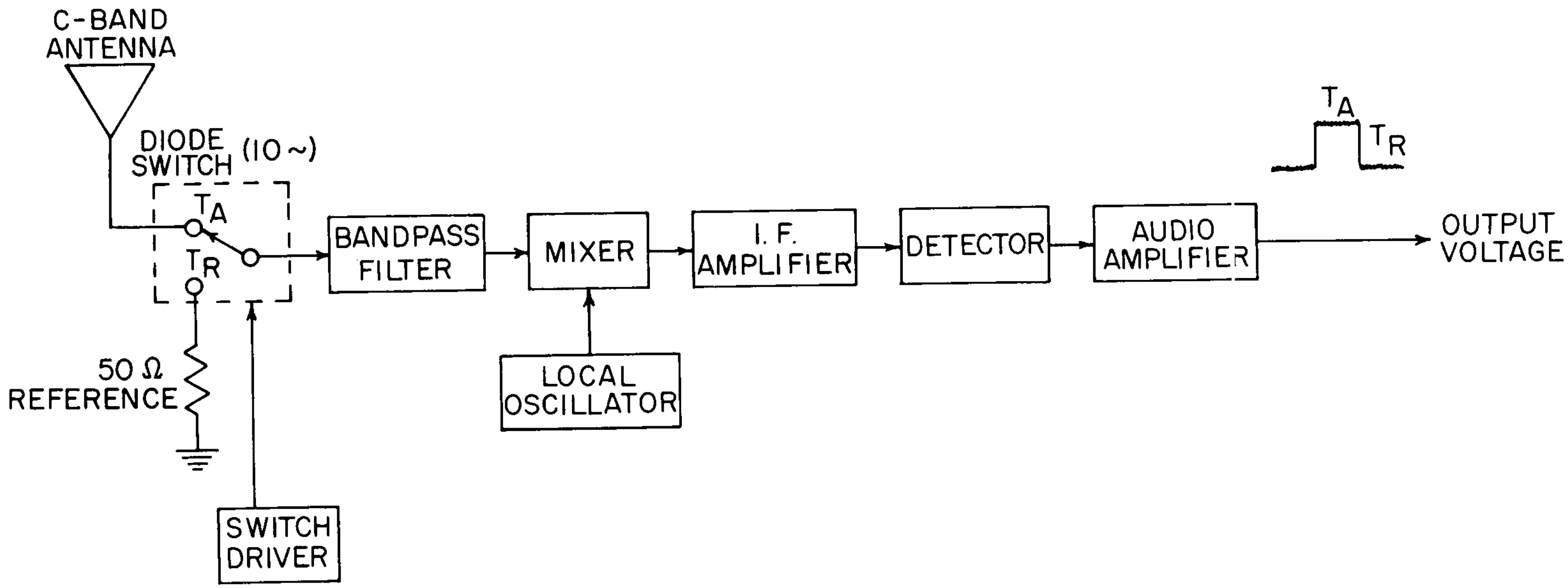

Figure 7.- Microwave radiometer system.

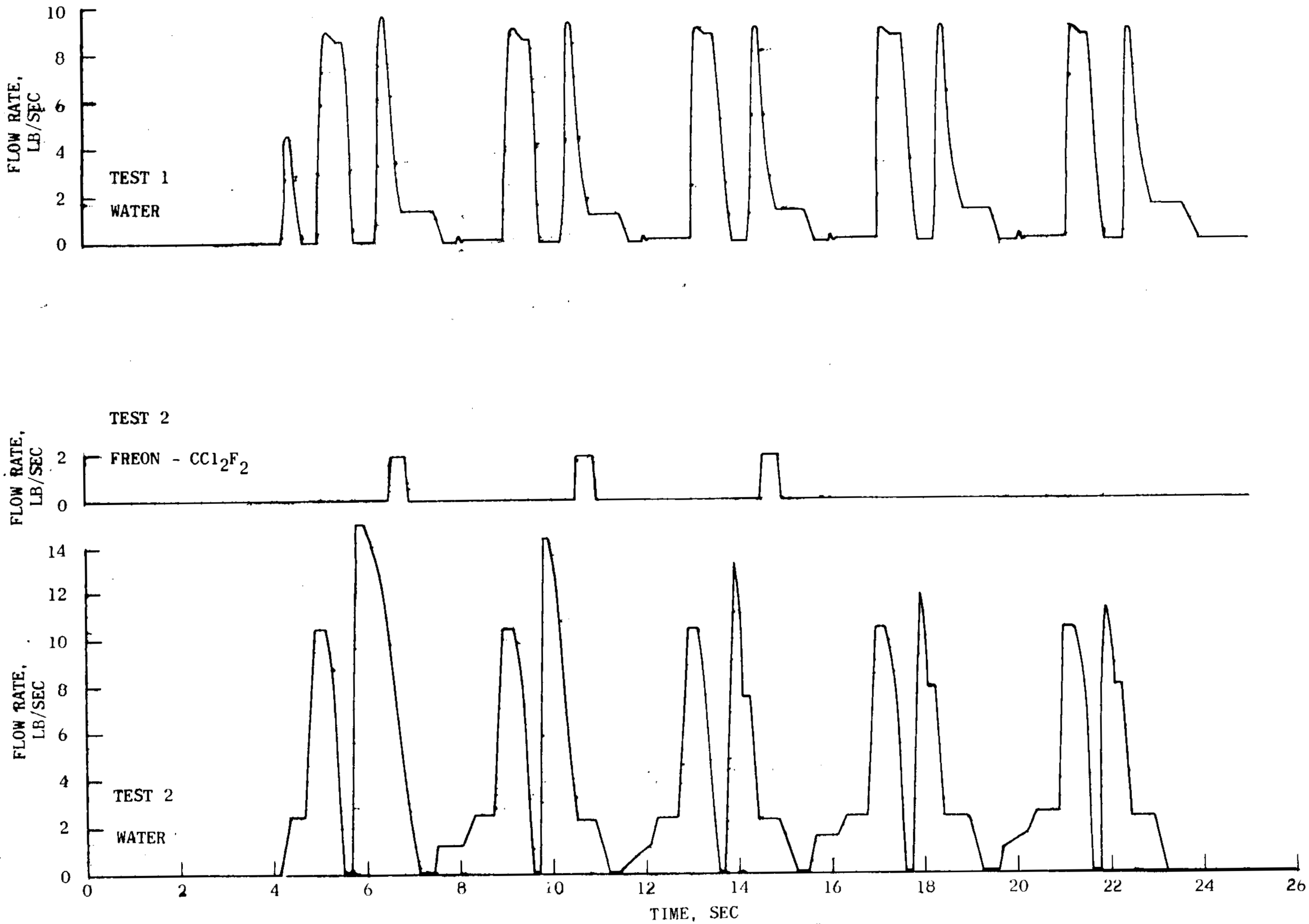

Figure 8.- Water and freon (CCl_2F_2) flow rates during motor operation.

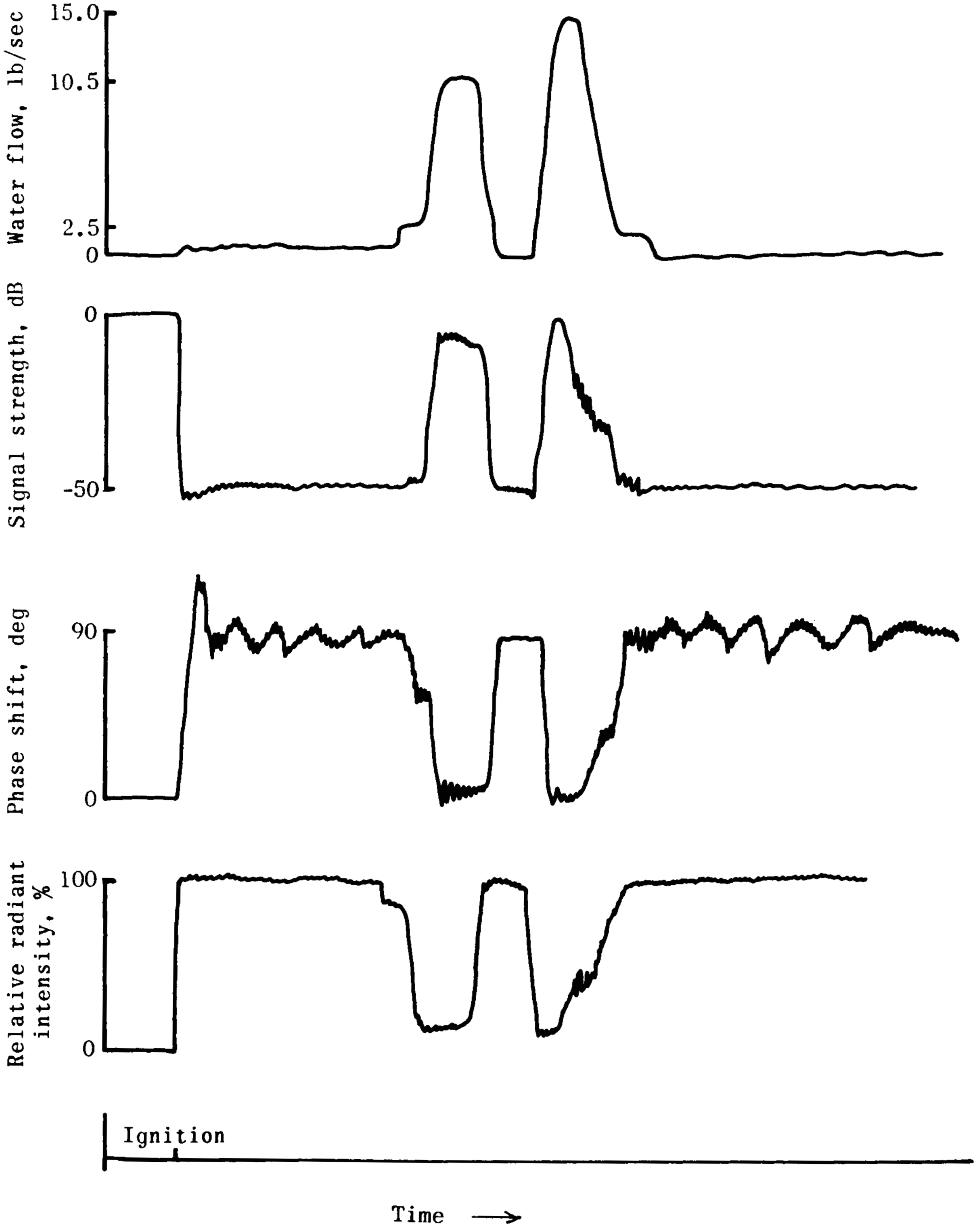

Figure 9.- Sample electromagnetic data during material injection.

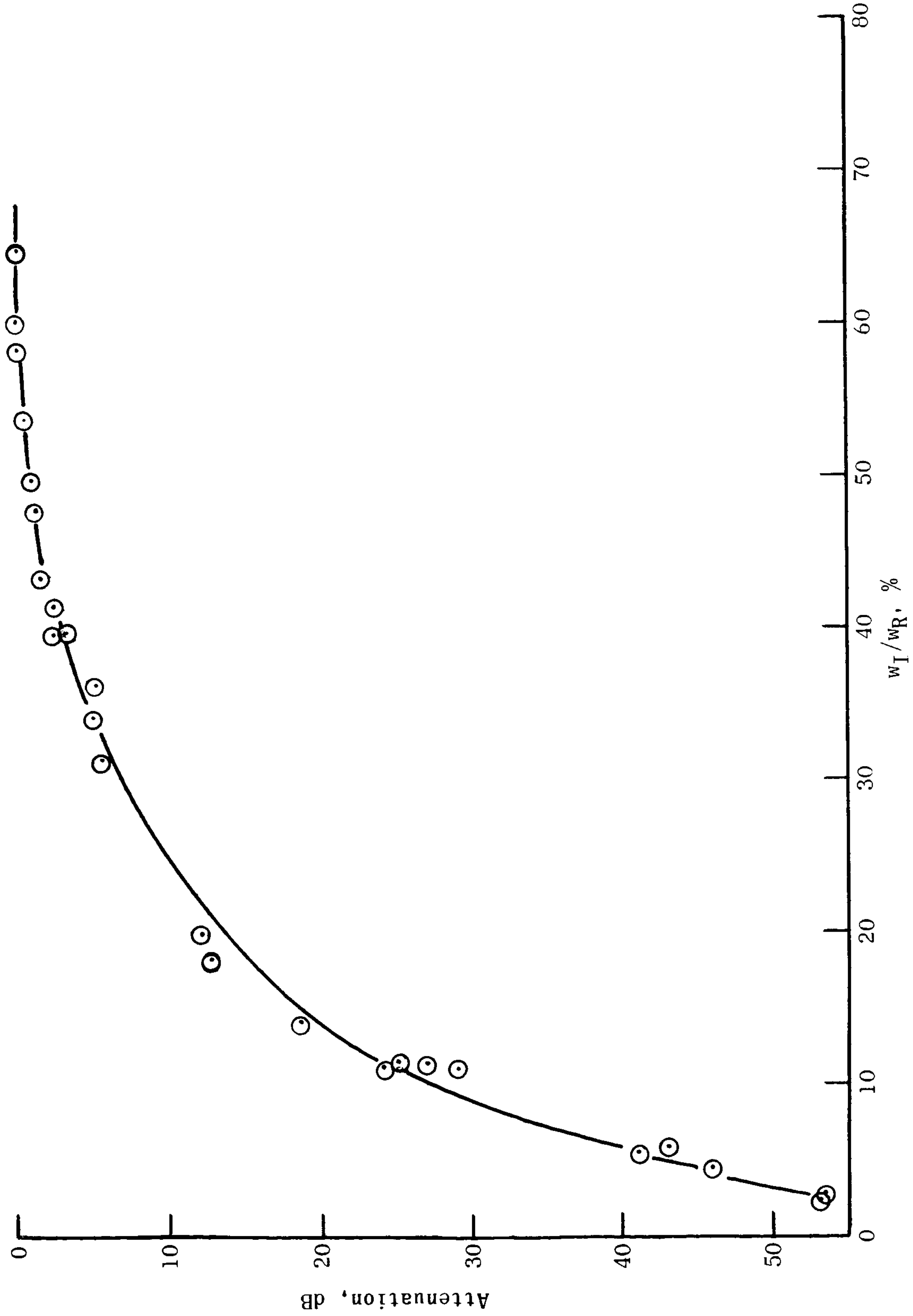

Figure 10.- X-band attenuation as a function of w_I/w_R.

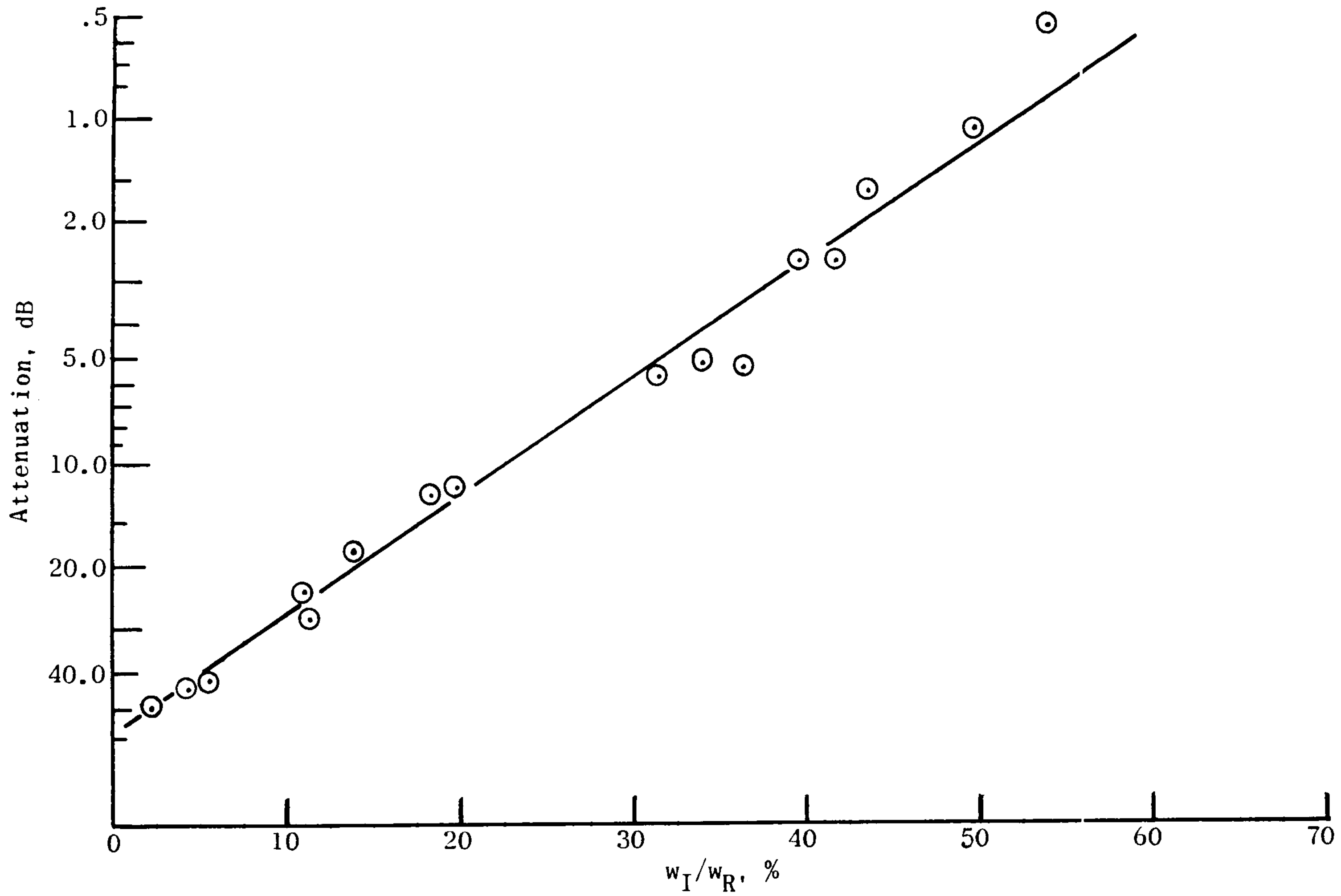

Figure 11.- Semilogarithmic plot of X-band attenuation as a function of w_I/w_R.

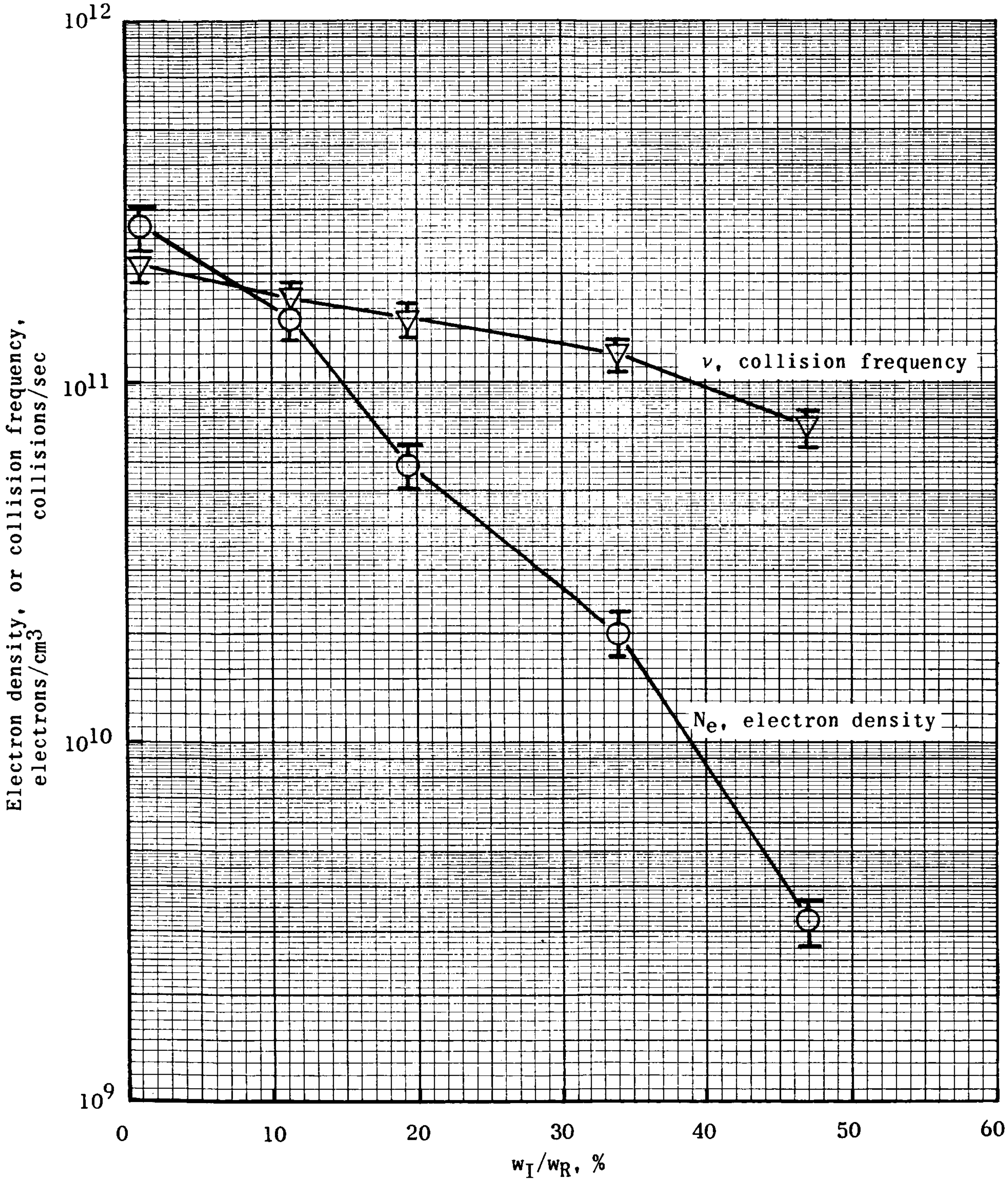

Figure 12.- Experimental exhaust plasma parameters calculated from X-band transmission data as a function of w_I/w_R.

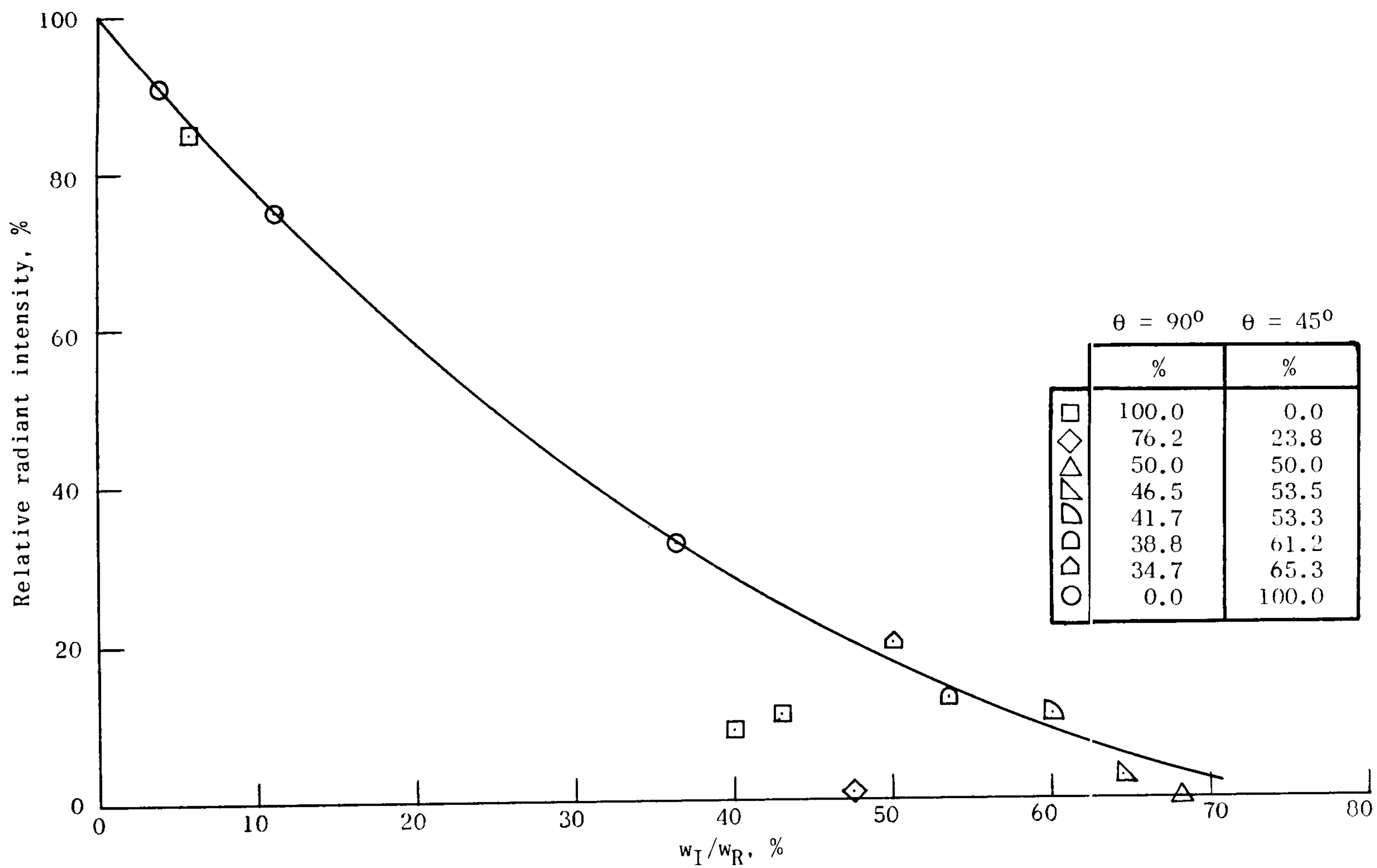

Figure 13.- Relative radiant intensity as a function of w_I/w_R.

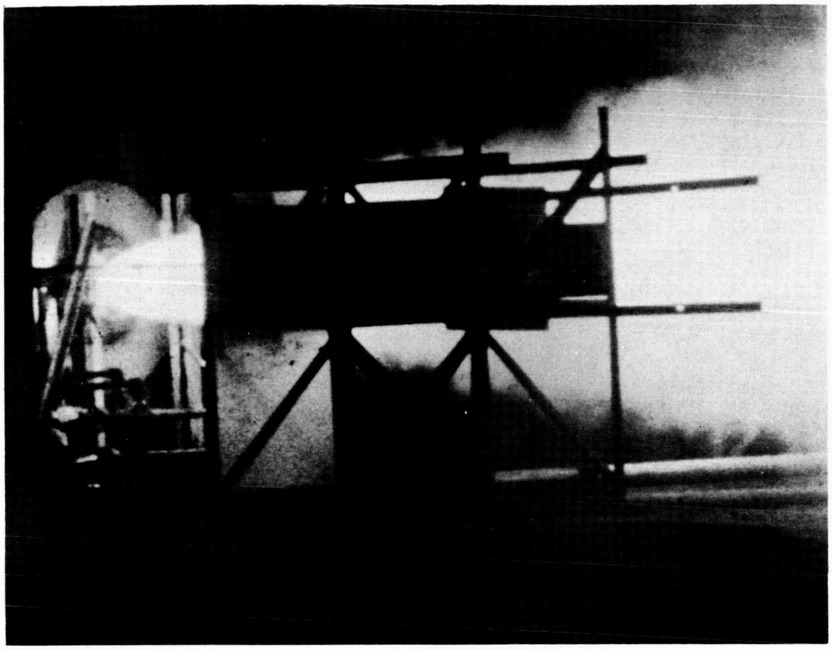

(a) Before injection.

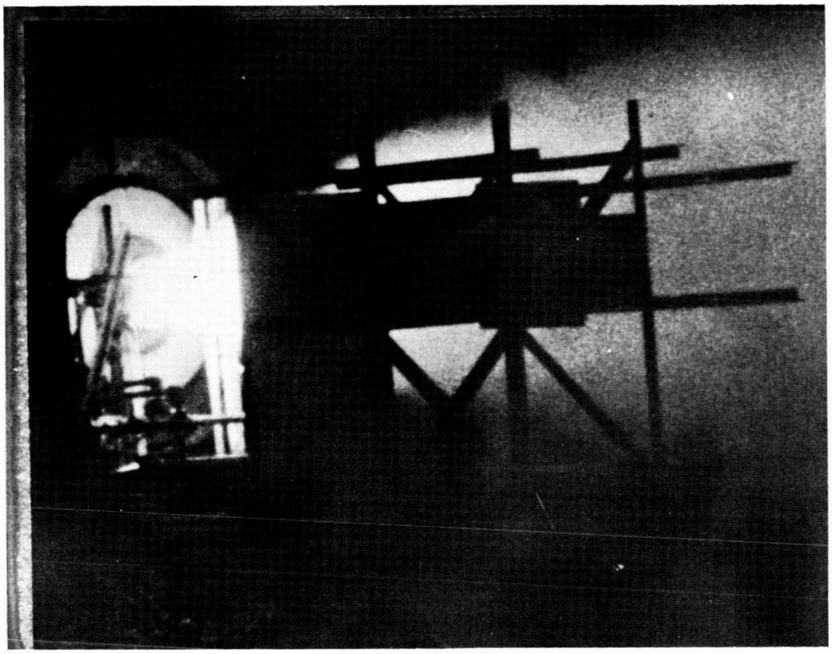

(b) During injection. L-64-4712

Figure 14.- Frames from motion pictures showing effect of injectant on luminosity.

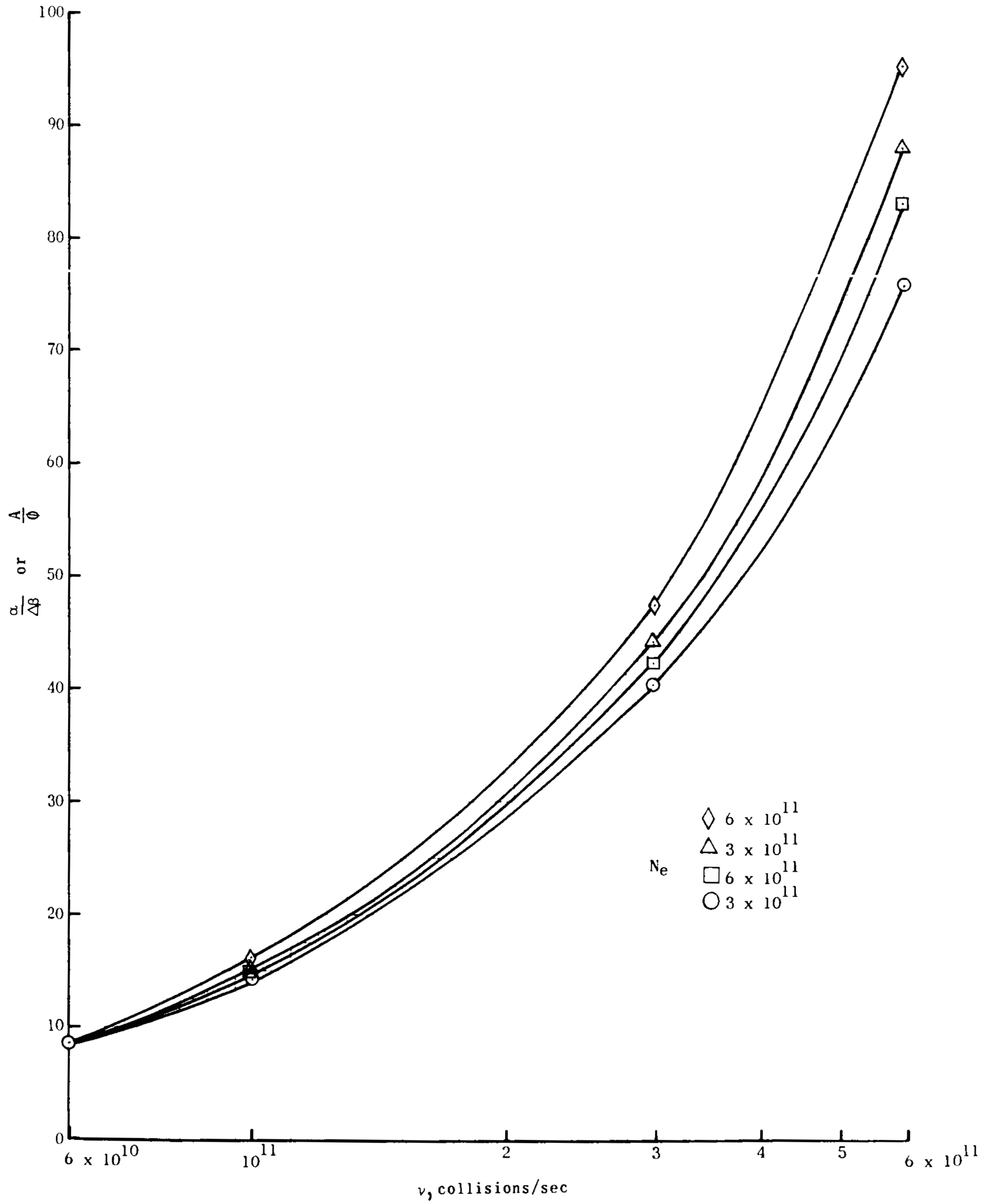

Figure 15.- Ratio of attenuation to phase shift as a function of electron collision frequency for several electron densities.

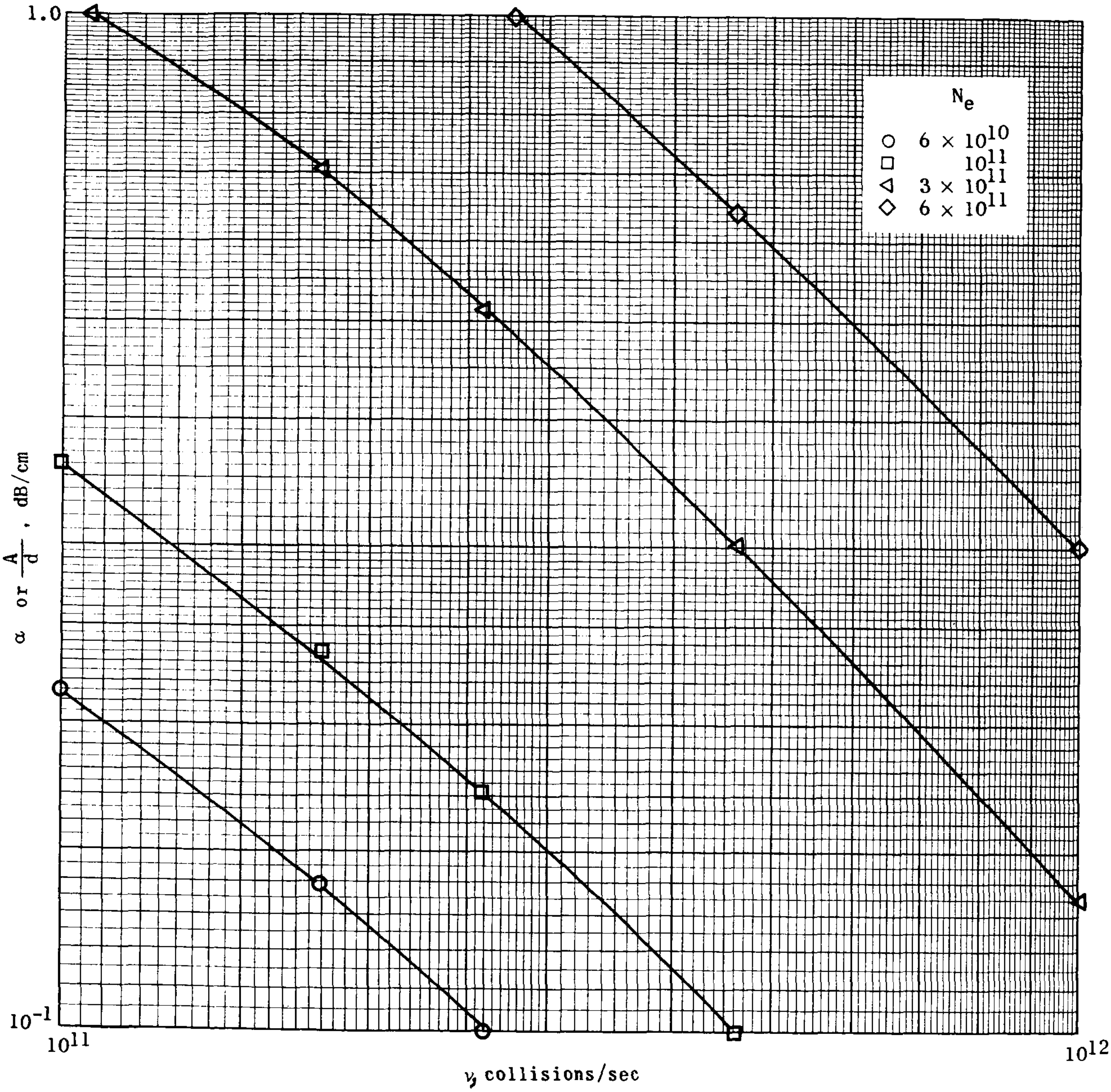

Figure 16.- Attenuation coefficient as a function of collision frequency for several electron densities.

NASA-Langley, 1965 L-3796

"The aeronautical and space activities of the United States shall be conducted so as to contribute . . . to the expansion of human knowledge of phenomena in the atmosphere and space. The Administration shall provide for the widest practicable and appropriate dissemination of information concerning its activities and the results thereof."

—NATIONAL AERONAUTICS AND SPACE ACT OF 1958

NASA SCIENTIFIC AND TECHNICAL PUBLICATIONS

TECHNICAL REPORTS: Scientific and technical information considered important, complete, and a lasting contribution to existing knowledge.

TECHNICAL NOTES: Information less broad in scope but nevertheless of importance as a contribution to existing knowledge.

TECHNICAL MEMORANDUMS: Information receiving limited distribution because of preliminary data, security classification, or other reasons.

CONTRACTOR REPORTS: Technical information generated in connection with a NASA contract or grant and released under NASA auspices.

TECHNICAL TRANSLATIONS: Information published in a foreign language considered to merit NASA distribution in English.

TECHNICAL REPRINTS: Information derived from NASA activities and initially published in the form of journal articles.

SPECIAL PUBLICATIONS: Information derived from or of value to NASA activities but not necessarily reporting the results of individual NASA-programmed scientific efforts. Publications include conference proceedings, monographs, data compilations, handbooks, sourcebooks, and special bibliographies.

Details on the availability of these publications may be obtained from:

SCIENTIFIC AND TECHNICAL INFORMATION DIVISION

NATIONAL AERONAUTICS AND SPACE ADMINISTRATION

Washington, D.C. 20546